

# Humic Acid Removal from Water by Iron-coated Sand: A Column Experiment

Hyon-Chong Kim, Seong-Jik Park, Chang-Gu Lee, Yong-Un Han, Jeong-Ann Park,  
and Song-Bae Kim<sup>†</sup>

*Environmental Biocolloid Engineering Laboratory, Department of Rural Systems Engineering, Seoul National University, Seoul 151-921, Korea*

*Received October 2008, accepted March 2009*

---

## Abstract

Column experiments were performed in this study to investigate humic acid adhesion to iron oxide-coated sand (ICS) under different experimental conditions including influent humic acid concentration, flow rate, solution pH, and ionic strength/composition. Breakthrough curves of humic acid were obtained by monitoring effluents, and then column capacity for humic acid adsorption ( $C_{cap}$ ), total adsorption percent ( $R$ ), and mass of humic acid adsorbed per unit mass of filter media ( $q_a$ ) were quantified from these curves. Results showed that humic acid adhesion was about seven times higher in ICS than in quartz sand at given experimental conditions. This indicates that humic acid removal can be enhanced through the surface charge modification of quartz sand with iron oxide coating. The adhesion of humic acid in ICS was influenced by influent humic acid concentration.  $C_{cap}$  and  $q_a$  increased while  $R$  decreased with increasing influent humic acid concentration in ICS column. However, the influence of flow rate was not eminent in our experimental conditions. The humic acid adhesion was enhanced with increasing salt concentration of solution.  $C_{cap}$ ,  $q_a$  and  $R$  increased in ICS column with increasing salt concentration. On the adhesion of humic acid, the impact of  $\text{CaCl}_2$  was greater than that of  $\text{NaCl}$ . Also, the humic acid adhesion to ICS decreased with increasing solution pH.  $C_{cap}$ ,  $q_a$  and  $R$  decreased with increasing solution pH. This study demonstrates that humic acid concentration, salt concentration/composition, and solution pH should be controlled carefully in order to improve the ICS column performance for humic acid removal from water.

*Keywords:* Humic acid adhesion, Quartz sand, Iron oxide-coated sand, Column experiment

---

## 1. Introduction

Natural organic matter is a complex mixture of compounds including humic substances, hydrophilic acids, amino acids, lipids, and proteins. Humic substances (humic acid, fulvic acid, humin) are major constituents of natural organic matter.<sup>1)</sup> They are found in varying concentrations in aquatic environments and present as dissolved molecules or colloidal/particulate forms.<sup>2)</sup> In environmental systems, humic substances play several significant roles related to water quality issues: i) producing disinfection by-products (DBPs) such as trihalomethanes (human carcinogens) by reacting with chlorine in water treatment, ii) enhancing the transport of hydrophobic organic contaminants or heavy metals by binding with them, iii) causing bacterial growth in water distribution systems by serving as food source, iv) inducing unpleasant taste and color in drinking water.<sup>3-6)</sup> It is, therefore, necessary to remove humic substances from water using effective treatment processes.

In conventional water treatment processes, chemical coagulation/flocculation has been widely applied to remove humic substances using metal salt coagulants (e.g. alum, ferric chloride). This process, however, generates a large volume of sludge and requires a high operational cost.<sup>7)</sup> As an alternative to coagulation/flocculation process, adsorptive filtration using granular media coated with metal oxyhydroxide has attracted considerable attention for humic substances removal. Humic substances are negatively-charged at circumneutral pH conditions due to the prevalence of carboxyl and phenol groups on their surface.<sup>8)</sup> Therefore, surface interactions between humic substances and sand are not favorable because both are like-charged such that sand filtration process is not effective in the removal of humic substances.<sup>6)</sup> However, surface charge modification of sand via metal oxyhydroxide coating generates positively-charged granular media, leading to favorable surface interactions between them. Even though several researchers have reported the interactions between humic substances and metal oxides in batch conditions,<sup>9-12)</sup> only few studies have been performed in column experiments to examine the adsorption of humic substances to coated-sand filter media,<sup>13,14)</sup> and their studies have focused on

---

<sup>†</sup> Corresponding author  
E-mail: songbkim@snu.ac.kr  
Tel: +82-2-880-4587, Fax: +82-2-873-2087

the effect of humic acid on the adsorption of metal ions to iron oxide-coated sand. Further experiments are required to improve knowledge regarding the adhesion of humic substances to coated-sand media.

Therefore, column experiments were performed in this study to investigate the adhesion of humic acid to iron oxide-coated sand under different experimental conditions including influent humic acid concentration, flow rate, solution pH, and ionic strength/composition. Breakthrough curves of humic acid were obtained by monitoring effluents, and then parameters related to column performance were quantified from these curves.

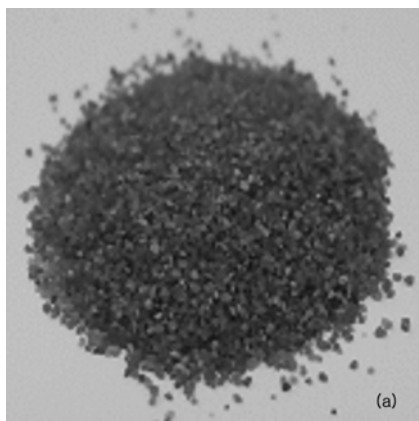
## 2. Material and Methods

### 2.1. Iron Oxide-coated Sand

Quartz sand (Jumunjin Silica, Korea) was used in the experiments. Mechanical sieving was conducted with US Standard Sieves (Fisher Scientific) Nos. 35 and 10. Sand fractions with a grain size of 0.5-2.0 mm were used to prepare the iron oxide-coated sand. Before use, sand was washed twice using deionized water to remove impurities on the surface, and wet sand was autoclaved for 20 min at 17.6 psi, cooled to room temperature, and oven-dried at 105°C for 1-2 days.

For the preparation of iron oxide-coated sand (ICS),  $\text{FeCl}_3 \cdot 6\text{H}_2\text{O}$  (5.5 g) was dissolved in deionized water (100 mL), and the solution pH was adjusted with 6N NaOH. The quartz sand (200 g) was added to the  $\text{FeCl}_3 \cdot 6\text{H}_2\text{O}$  solution and then mixed in a rotary evaporator (90°C, 80 rpm, 20 min) to remove water in the suspension by heating (Hahn vapor, Hahnshin Scientific Co., Korea). The coated sand was dried at 150° for 6 hr, washed with deionized water, and then dried again at the same conditions (Fig. 1(a)). Scanning electron microscopy (SEM) analysis along with Energy Dispersive X-ray Spectrometer (EDS) analysis were performed to examine the presence of Fe on the coated sand using a scanning electron microscope (JSM 5410LV, JEOL, Japan). The SEM images and EDS patterns have been reported elsewhere.<sup>15)</sup>

### 2.2. Column Experiments



Column experiments were performed at different conditions (Table 1 and 2) using a Plexiglas column (inner diameter 2.5 cm, bed depth 10 cm, bulk volume 49.1 cm<sup>3</sup>) packed with quartz sand or ICS (mass of filter media 77.2 g, bed porosity 0.407, fixed-bed volume 20.0 cm<sup>3</sup>). Stock solutions of humic acid were prepared by dissolving appropriate amounts of humic acid (Sodium salt, Tech., Aldrich Chemical, USA) in deionized water (Fig. 1(b)). Prior to the experiments, the packed column was flushed upward using a HPLC pump (Series II pump, Scientific Systems Inc., USA) with 15-20 bed volumes (BV) of leaching solution until the column effluents were clear ( $\approx 0.0 \text{ OD}_{254}$ ) and a steady state flow condition was established. Then, humic acid solution was introduced downward to the packed column. The pH of injected humic acid solution was adjusted using 1M HCl and/or 1M NaOH. Portions of the effluent were collected using the auto collector (Retriever 500, Teledyne, USA) at a regular interval, and the concentrations of humic acid were determined at 254 nm using a UV-spectrophotometer (Helios, Thermo, USA).

### 2.3. Data Analysis

The empty bed contact time (EBCT, min) can be determined as following:

$$\text{EBCT} = \frac{V_r}{Q} \quad (1)$$

where  $V_r$  is the fixed-bed volume (cm<sup>3</sup>), and  $Q$  is the volumetric flow rate (mL/min). The total mass of humic acid injected into column ( $M_{total}$ , mg) during the experiment can be calculated as following:

$$M_{total} = \frac{C_0 Q t_{total}}{1000} \quad (2)$$

where  $C_0$  is the influent concentration of humic acid (mg/L), and  $t_{total}$  is the total flow time (min). The column capacity for

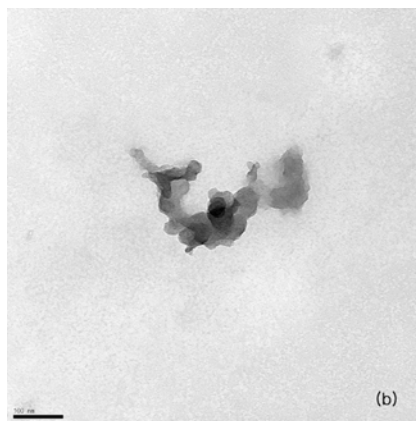


Fig. 1. Images of (a) iron-coated sand (photo image) and (b) humic acid (transmission electron microscope image) used in the experiment.

Table 1. Experimental conditions and results for humic acid adhesion to quartz sand and iron oxide-coated sand (ICS) (solution pH: 7.1-7.3)

| Ex  | Filter media | Solution                   | $C_0$<br>(mg/L) | $Q$<br>(mL/min) | EBCT<br>(min) | $M_{total}$<br>(mg) | $C_{cap}$<br>(mg) | $R$<br>(%) | $q_a$<br>(mg/g) |
|-----|--------------|----------------------------|-----------------|-----------------|---------------|---------------------|-------------------|------------|-----------------|
| a1  | Quartz       | DW*                        | 25              | 1.0             | 20            | 22.13               | 0.64              | 2.9        | 0.008           |
| a2  | Quartz       | NaNO <sub>3</sub> 0.25 mM  | 25              | 1.0             | 20            | 22.13               | 0.91              | 4.1        | 0.012           |
| a3  | Quartz       | NaNO <sub>3</sub> 0.5 mM   | 25              | 1.0             | 20            | 22.13               | 1.10              | 5.0        | 0.014           |
| a4  | ICS          | DW                         | 10              | 1.0             | 20            | 8.85                | 2.98              | 33.6       | 0.039           |
| a5  | ICS          | DW                         | 25              | 4.0             | 5             | 22.13               | 3.27              | 14.8       | 0.042           |
| a6  | ICS          | DW                         | 25              | 2.0             | 10            | 22.13               | 3.33              | 15.1       | 0.043           |
| a7  | ICS          | DW                         | 25              | 1.0             | 20            | 22.13               | 4.45              | 20.1       | 0.058           |
| a8  | ICS          | DW                         | 50              | 1.0             | 20            | 44.25               | 5.47              | 12.4       | 0.071           |
| a9  | ICS          | NaNO <sub>3</sub> 0.25 mM  | 25              | 1.0             | 20            | 22.13               | 6.25              | 28.2       | 0.081           |
| a10 | ICS          | NaNO <sub>3</sub> 0.5 mM   | 25              | 1.0             | 20            | 22.13               | 6.86              | 31.0       | 0.089           |
| a11 | ICS          | NaCl 0.125 mM              | 25              | 1.0             | 20            | 22.13               | 4.88              | 22.1       | 0.063           |
| a12 | ICS          | NaCl 0.25 mM               | 25              | 1.0             | 20            | 22.13               | 5.49              | 24.8       | 0.071           |
| a13 | ICS          | NaCl 0.5 mM                | 25              | 1.0             | 20            | 22.13               | 6.51              | 29.4       | 0.084           |
| a14 | ICS          | CaCl <sub>2</sub> 0.125 mM | 25              | 1.0             | 20            | 22.13               | 13.22             | 59.8       | 0.171           |
| a15 | ICS          | CaCl <sub>2</sub> 0.25 mM  | 25              | 1.0             | 20            | 22.13               | 14.62             | 66.1       | 0.189           |
| a16 | ICS          | CaCl <sub>2</sub> 0.5 mM   | 25              | 1.0             | 20            | 22.13               | 16.26             | 73.5       | 0.211           |

\* deionized water

Table 2. Experimental conditions and results for humic acid attachment to quartz and iron-coated sands (ICS) at different solution pHs (ionic strength = 100 mM NaNO<sub>3</sub>)

| Ex | Media  | pH  | $C_0$<br>(mg/L) | $Q$<br>(mL/min) | EBCT<br>(min) | $M_{total}$<br>(mg) | $C_{cap}$<br>(mg) | $R$<br>(%) | $q_a$<br>(mg/g) |
|----|--------|-----|-----------------|-----------------|---------------|---------------------|-------------------|------------|-----------------|
| b1 | Quartz | 6.1 | 25              | 2.0             | 10            | 114.63              | 4.74              | 4.1        | 0.061           |
| b2 | Quartz | 6.6 | 25              | 2.0             | 10            | 114.63              | 2.48              | 2.2        | 0.032           |
| b3 | Quartz | 7.3 | 25              | 2.0             | 10            | 114.63              | 2.34              | 2.0        | 0.030           |
| b4 | ICS    | 5.9 | 25              | 2.0             | 10            | 114.63              | 31.51             | 27.5       | 0.408           |
| b5 | ICS    | 6.7 | 25              | 2.0             | 10            | 114.63              | 24.99             | 21.8       | 0.324           |
| b6 | ICS    | 7.1 | 25              | 2.0             | 10            | 114.63              | 19.98             | 17.4       | 0.259           |

humic acid adsorption at a given flow rate and influent concentration of humic acid ( $C_{cap}$ , mg) can be quantified as following:

$$C_{cap} = \frac{Q}{1000} \int_{t=0}^{t=t_{total}} (C_0 - C) dt \quad (3)$$

where  $C$  is the effluent concentration of humic acid (mg/L). The total adsorption percent of humic acid during the experiment ( $R$ , %) can be calculated as following:

$$R = \left( \frac{C_{cap}}{M_{total}} \right) \times 100 \quad (4)$$

The mass of humic acid adsorbed per unit (dry) mass of filter media in the column ( $q_a$ , mg/g) can be determined as following:

$$q_a = \frac{C_{cap}}{M_f} \quad (5)$$

where  $M_f$  is the mass of filter media in the column (g).

### 3. Results and Discussion

#### 3.1. Humic Acid Adhesion to Iron Oxide-coated Sand

The breakthrough curves (BTCs) for humic acid adhesion to quartz sand (a1) and ICS (a7) are presented in Fig. 2. The breakthrough data is presented in terms of relative concentration ( $C/C_0$ ) versus BV. At the given conditions ( $C_0 = 25$  mg/L,  $Q = 1.0$  mL/min) in quartz sand, the BTC increased sharply, reaching to  $C/C_0 = 1.0$  at 3.8 BV. At the same experimental conditions, the BTC in ICS was delayed relative to the BTC in quartz sand. Also, it increased rapidly up to 10 BV ( $C/C_0 = 0.79$ ) and did slowly thereafter, reaching to  $C/C_0 = 0.90$  around 45 BV. In quartz sand ( $C_0 = 25$  mg/L,  $Q = 1.0$  mL/min),  $C_{cap}$  was 0.64 mg while it was 4.45 mg in ICS, which is about seven times higher than that of quartz sand. The values of  $R$  in quartz sand and ICS were 2.9 and 20.1%, respectively. In addition,  $q_a$  was 0.008 mg/g in quartz sand while it was 0.058 mg/g in ICS.

The enhancement of humic acid adhesion through the surface charge modification of quartz sand with iron oxide coating may be explained by the point of zero charge ( $pH_{pzc}$ ) of porous media. The  $pH_{pzc}$  is the pH where net surface charge is equal to zero. The surface charges of porous media depend on the solution

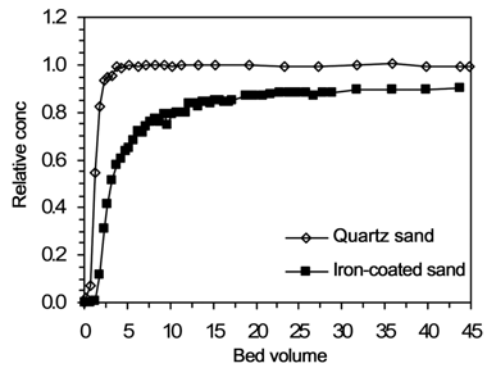


Fig. 2. Breakthrough curves for humic acid adhesion to quartz sand and iron oxide-coated sand ( $C_0 = 25$  mg/L and  $Q = 1.0$  mL/min).

pH. The porous media carry positive charges below the  $\text{pH}_{\text{pzc}}$  but negative charges above it. The  $\text{pH}_{\text{pzc}}$  of quartz sand is 2.0,<sup>16)</sup> and so quartz sand is negatively charged at circumneutral pH. Humic acid is also negatively-charged at circumneutral pH due to the prevalence of carboxyl and phenol groups on their surface.<sup>8)</sup> Thus, the electrostatic interaction between quartz sand and humic acid is repulsive in our experimental condition. Meanwhile, the  $\text{pH}_{\text{pzc}}$  of iron oxide-coated sand is around 8.0.<sup>17)</sup> Therefore, the electrostatic interaction between iron oxide-coated sand and humic acid is attractive in our condition, resulting in the enhancement of humic acid adhesion.

### 3.2. Effects of Humic Acid Concentration and Flow Rate

The BTCs for humic acid adhesion to ICS at different influent concentrations of humic acid (a4, a7, a8) are presented in Fig. 3(a). At the given condition ( $Q = 1.0$  mL/min), the BTC was slightly delayed and lowered as the influent concentration decreased.  $C_{\text{cap}}$  increased as  $C_0$  increased. At  $C_0 = 10$  mg/L,  $C_{\text{cap}}$  was 2.98 mg and increased to 4.45 mg at  $C_0 = 25$  mg/L and further to 5.47 mg at  $C_0 = 50$  mg/L. This can be attributed to the total mass of humic acid injected into column ( $M_{\text{total}}$ ) during the experiment (45 BV).  $M_{\text{total}}$  was 8.85 mg at  $C_0 = 10$  mg/L and increased to 22.13 mg at  $C_0 = 25$  mg/L and further to 44.25 mg at  $C_0 = 50$  mg/L.  $q_a$  also increased with increasing  $C_0$ . The values of  $q_a$  were 0.039, 0.058, and 0.071 mg/g for  $C_0 = 10, 25,$  and 50 mg/L, respectively. Meanwhile,  $R$  decreased with increasing  $C_0$ . The values of  $R$  were 33.6, 20.1, and 12.4% for  $C_0 = 10, 25,$  and 50 mg/L, respectively. It indicates that the influent humic acid concentration is an important factor, determining the ICS column performance for humic acid adhesion.

The BTCs for humic acid adhesion to ICS at different flow rates (or EBCTs) (a5, a6, a7) are presented in Fig. 3(b). All BTCs increased rapidly up to 10 BV, followed by slow increment. The BTC was slightly lowered as the flow rate decreased from 4.0 to 1.0 mL/min (or EBCT increased from 5 to 20 min).  $C_{\text{cap}}$  increased with increasing EBCT. The values of  $C_{\text{cap}}$  were in the range from 3.27 to 4.45 mg. As the EBCT increased,  $R$  also increased from 14.8 to 20.1%. In addition,  $q_a$  increased from 0.042 to 0.058 mg/g. It indicates that the impact of flow rate (or EBCT) on the adhesion of humic acid in ICS was not eminent in our experimental conditions even though slight

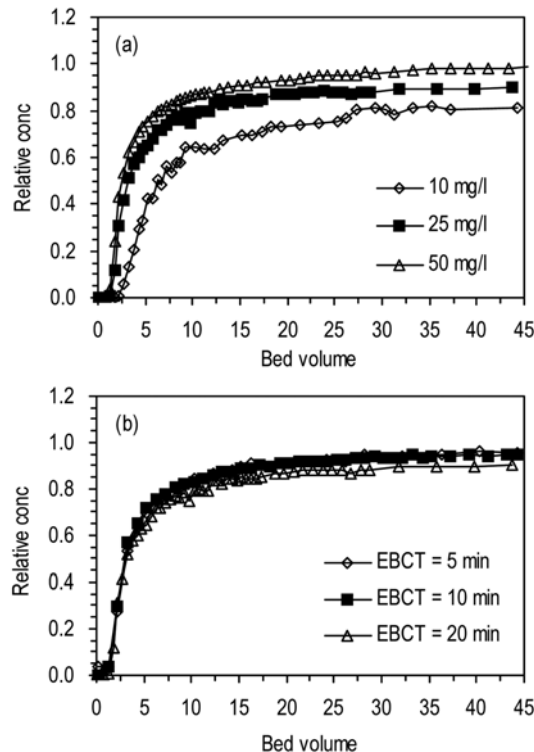


Fig. 3. Breakthrough curves for humic acid adhesion to iron oxide-coated sand (a) at different influent concentrations of humic acid ( $Q = 1.0$  mL/min) and (b) at different flow rates (or empty bed contact times, EBCTs) ( $C_0 = 25$  mg/L).

enhancement in humic acid adhesion was observed with increasing EBCT in the experiments.

### 3.3. Effect of Salt Concentration

The BTCs for humic acid adhesion to quartz sand and ICS at different  $\text{NaNO}_3$  concentration are presented in Fig. 4. With increasing concentration of  $\text{NaNO}_3$ , the BTC was slightly delayed and lowered. In quartz sand (a1, a2, a3),  $C_{\text{cap}}$  and  $R$  increased from 0.64 to 1.10 mg and from 2.9 to 5.0%, respectively, with increasing  $\text{NaNO}_3$  concentration from 0 to 0.5 mM.  $q_a$  increased from 0.008 to 0.014 mg/g. In ICS (a7, a9, a10),  $C_{\text{cap}}$  and  $R$  increased from 4.45 to 6.86 mg and from 20.1 to 31.0%, respectively, with increasing  $\text{NaNO}_3$  concentration from 0 to 0.5 mM.  $q_a$  increased from 0.058 to 0.089 mg/g.

The BTCs for humic acid adhesion to ICS at different concentrations of  $\text{NaCl}$  and  $\text{CaCl}_2$  are presented in Fig. 5. In the solution of  $\text{NaCl}$  (a7, a11, a12, a13), the BTC was slightly delayed and lowered as the salt concentration increased from 0 to 0.5 mM (Fig. 5(a)). In the case of  $\text{CaCl}_2$  solution (a7, a14, a15, a16), the magnitude of impact of salt concentration on humic acid adhesion was greater than that of  $\text{NaCl}$ . With increasing concentration of  $\text{CaCl}_2$  from 0 to 0.5 mM (Fig. 5(b)), the BTC was markedly delayed and lowered. In the solution of  $\text{NaCl}$ ,  $C_{\text{cap}}$  increased with increasing salt concentration from 0 to 0.5 mM. The values of  $C_{\text{cap}}$  were in the range between 4.45 and 6.51 mg. With increasing salt concentration,  $R$  also increased from 20.1 to 29.4%. In addition,  $q_a$  also increased from 0.058

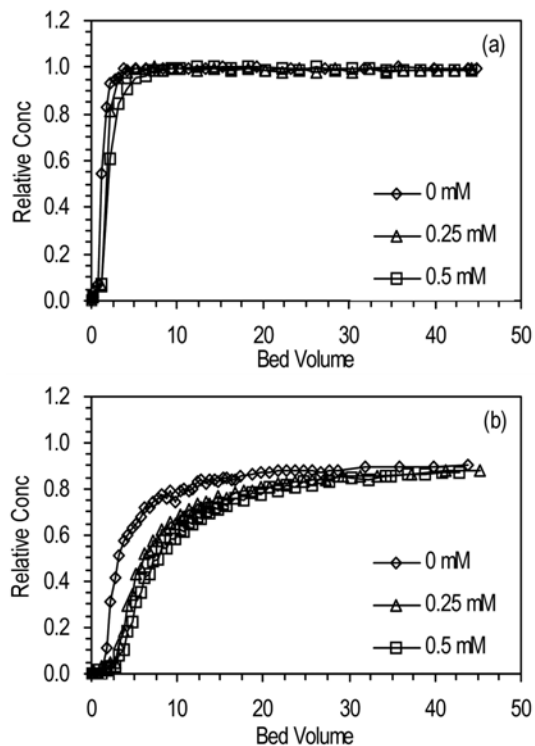


Fig. 4. Breakthrough curves for humic acid in (a) quartz and (b) iron-coated sands at different concentrations of  $\text{NaNO}_3$  ( $C_0 = 25 \text{ mg/L}$  and  $Q = 1.0 \text{ mL/min}$ ).

to  $0.084 \text{ mg/g}$ . In the solution of  $\text{CaCl}_2$ ,  $C_{cap}$  increased from  $4.45$  to  $16.26 \text{ mg}$ ,  $R$  from  $20.1$  to  $73.5\%$ , and  $q_a$  from  $0.058$  to  $0.211 \text{ mg/g}$ .

The enhancement of humic acid adhesion with increasing salt concentration may be explained by the screening effect of salt ions and compact conformation of humic acid.<sup>18)</sup> With increasing salt concentration, the electrostatic repulsion between the negatively-charged humic acid particles may be screened more effectively, resulting in the enhancement of humic acid adhesion to iron oxide-coated sand.<sup>19)</sup> In addition, the conformation of humic acid may become more compact (size reduction) with increasing salt concentration, leading to enhanced adsorption of humic acid to the media.<sup>12,20)</sup> That is, a larger fraction of humic acid may adsorb to the surfaces of coated sand due to compaction of humic acid particles at higher ionic strength than at lower ionic strength where the particles are more swelled.<sup>20)</sup> Our result is consistent with the report<sup>21)</sup> which has shown with a batch experiment that the adsorbed humic acid onto goethite increased with increasing concentration of  $\text{NaNO}_3$  from  $0.002$  to  $0.1 \text{ M}$ . Other studies<sup>19,20)</sup> have also reported the enhanced adsorption of humic acid onto goethite or iron oxide particles with increasing salt concentration. Our result also indicates that the impact of  $\text{CaCl}_2$  was greater than those of  $\text{NaCl}$  on the adhesion of humic acid. This phenomenon may be attributed to formation of bridges by a divalent ion  $\text{Ca}^{2+}$  between humic acid and iron oxide surface and/or complexation of functional groups of humic acid with  $\text{Ca}^{2+}$ .<sup>18,22)</sup> Also, it may be attributed to the increased ionic strength through the addition of  $\text{CaCl}_2$  relative to  $\text{NaCl}$ . At the same molar salt concentration the ionic strength of  $\text{CaCl}_2$  is three

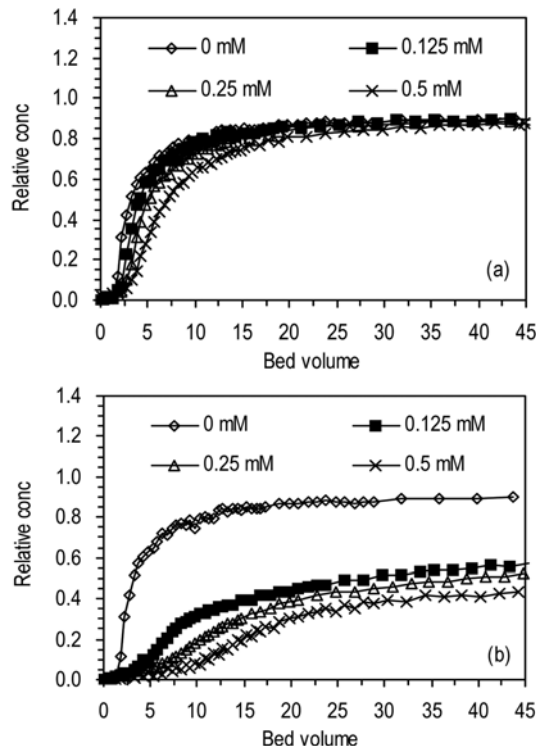


Fig. 5. Breakthrough curves for humic acid adhesion to iron oxide-coated sand ( $C_0 = 25 \text{ mg/L}$  and  $Q = 1.0 \text{ mL/min}$ ) at different concentrations of (a)  $\text{NaCl}$  and (b)  $\text{CaCl}_2$ .

times larger than that of  $\text{NaCl}$ , which results in the enhancement of humic acid adhesion.

### 3.4. Effect of Solution pH

The BTCs for humic acid adhesion to quartz sand and ICS at different solution pHs are presented in Fig. 6. With increasing pH, the BTC was delayed and lowered in ICS. But, the impact of pH on the BTC was minimal in quartz sand in given experimental conditions. In quartz sand (b1, b2, b3),  $C_{cap}$  slightly decreased from  $4.74$  to  $2.34 \text{ mg}$ ,  $R$  from  $4.1$  to  $2.0\%$ , and  $q_a$  from  $0.061$  to  $0.030 \text{ mg/g}$ , respectively, with increasing pH from  $6.1$  to  $7.3$ . In ICS (b4, b5, b6),  $C_{cap}$ ,  $R$ , and  $q_a$  decreased from  $31.51$  to  $19.98 \text{ mg}$ , from  $27.5$  to  $17.4\%$ , and from  $0.408$  to  $0.259 \text{ mg/g}$ , respectively.

Our result is consistent with the result of other researcher<sup>14)</sup> who have reported that the adsorption of humic acid onto ICS decreased from  $0.31$  to  $0.07 \text{ mg/g}$  with increasing pH from  $2.5$  to  $7.5$ . This result can be attributed to the change of ICS surface charge. As the pH approaches to  $\text{pH}_{\text{pzc}}$ , the strength of positive charge of ICS diminishes, resulting in the reduction of electrostatic attraction between humic acid and ICS.<sup>14)</sup>

## 4. Conclusions

Column experiments were performed to investigate humic acid adhesion to ICS. Results showed that humic acid adhesion was about seven times higher in ICS than in quartz sand at given experimental conditions. This indicates that humic acid removal

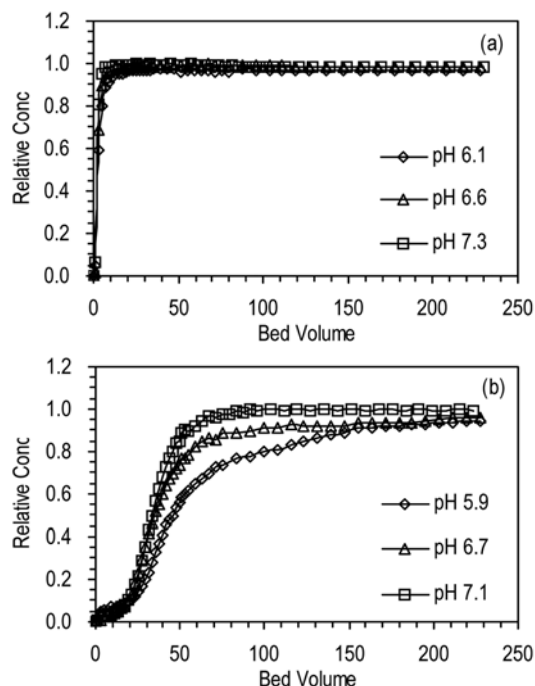


Fig. 6. Breakthrough curves for humic acid in (a) quartz and (b) iron-coated sands at different solution pHs ( $C_0 = 25$  mg/L and  $Q = 2.0$  mL/min).

can be enhanced through the surface charge modification of quartz sand with iron oxide coating. The adhesion of humic acid in ICS was influenced by influent humic acid concentration. However, the influence of flow rate (or EBCT) was not eminent in our experimental conditions. The humic acid adhesion was enhanced with increasing salt concentration of solution. On the adsorption of humic acid, the impact of  $\text{CaCl}_2$  was greater than that of  $\text{NaCl}$ . Also, the humic acid adhesion to ICS decreased with increasing solution pH. This study demonstrates that humic acid concentration, salt concentration/composition and solution pH should be controlled carefully in order to improve the ICS column performance for humic acid removal from water.

## References

1. Teermann, I. P. and Jekel, M. R., "Adsorption of humic substances onto  $\beta$ -FeOOH and its chemical regeneration," *Water Sci. Technol.*, **40**, 199-206 (1999).
2. Wilding, A., Liu, R., and Zhou, J. L., "Dynamic behaviour of river colloidal and dissolved organic matter through cross-flow ultrafiltration system," *J. Colloid Interf. Sci.*, **287**, 152-158 (2005).
3. Alborzfar, M., Jonsson, G., and Grøn, C., "Removal of natural organic matter from two types of humic ground waters by nanofiltration," *Water Res.*, **32**, 2983-2994 (1998).
4. Hong, S., "The role of pH and initial concentration on GAC adsorption for removal of natural organic matter," *Environ. Eng. Res.*, **3**, 183-190 (1998).
5. Balnois, E., Wilkinson, K. J., Lead, J. R., and Buffle, J., "Atomic force microscopy of humic substances: effects of pH and ionic strength," *Environ. Sci. Technol.*, **33**, 3911-3917 (1999).
6. Bai, R. and Zhang, X., "Polypyrrole-coated granules for humic acid removal," *J. Colloid Interf. Sci.*, **243**, 52-60 (2001).
7. Murray, C. A. and Parsons, S. A., "Preliminary laboratory investigation of disinfection by-product precursor removal using an advanced oxidation process," *Water Environ. J.*, **20**, 123-129 (2006).
8. Fein, J. B., Boily, J.-F., Güçlü, K., and Kaulbach, E., "Experimental study of humic acid adsorption onto bacteria and Al-oxide mineral surfaces," *Chem. Geol.*, **162**, 33-45 (1999).
9. Gu, B., Schmitt, J., Chen, Z., Liang, L., and McCarthy, J. F., "Adsorption and desorption of different organic matter fractions on iron oxide," *Geochim. Cosmochim. Acta*, **59**, 219-229 (1995).
10. Filius, J. D., Lumsdon, D. G., Meeussen, J. C. L., Hiemstra, T., and Van Riemsdijk, W. H., "Adsorption of fulvic acid on goethite," *Geochim. Cosmochim. Acta*, **64**, 51-60 (2000).
11. Fu, H. and Quan, X., "Complexes of fulvic acid on the surface of hematite, goethite, and akaganeite: FTIR observation," *Chemosphere*, **63**, 403-410 (2006).
12. Weng, L., van Riemsdijk, W. H., and Hiemstra, T., "Adsorption of humic acids onto goethite: effects of molar mass, pH and ionic strength," *J. Colloid Interf. Sci.*, **314**, 107-118 (2007).
13. Lai, C. H. and Chen, C. Y., "Removal of metal ions and humic acid from water by iron-coated filter media," *Chemosphere*, **44**, 1177-1184 (2001).
14. Lai, C. H., Chen, C. Y., Wei, B. L., and Yeh, S. H., "Cadmium adsorption on goethite-coated sand in the presence of humic acid," *Water Res.*, **36**, 4943-4950 (2002).
15. Kim, S. B., Park, S. J., Lee, C. G., Choi, N. C., and Kim, D. J., "Bacteria transport through goethite-coated sand: effects of solution pH and coated sand content," *Colloids Surf. B*, **63**, 236-242 (2008).
16. Scholl, M. A., Mills, A. L., Herman, J. S., and Hornberger, G. M., "The influence of mineralogy and solution chemistry on the attachment of bacteria to representative aquifer materials," *J. Contam. Hydrol.*, **6**, 321-336 (1990).
17. Ams, D. A., Fein, J. B., Dong, H., and Maurice, P. A., "Experimental measurements of the adsorption of *Bacillus subtilis* and *Pseudomonas mendocina* onto Fe-oxyhydroxide-coated and uncoated quartz grains," *Geomicrobiol. J.*, **21**, 511-519 (2004).
18. Kilduff, J. E. and Karanfil, T., "Trichloroethylene adsorption by activated carbon preloaded with humic substances: effects of solution chemistry," *Water Res.*, **36**, 1685-1698 (2002).
19. Saito, T., Koopal, L. K., van Riemsdijk, W. H., Nagasaki, S., and Tanaka, S., "Adsorption of humic acid on goethite: isotherms, charge adjustments, and potential profiles," *Langmuir*, **20**, 689-700 (2004).
20. Kim, E. K. and Walker, H. W., "Effect of cationic polymer additives on the adsorption of humic acid onto iron oxide particles," *Colloid. Surf. A*, **194**, 123-131 (2001).
21. Weng, L., van Riemsdijk, W. H., Koopal, L. K., and Hie-

- mstra, T., "Adsorption of humic substances onto goethite: comparison between humic acids and fulvic acids," *Environ. Sci. Technol.*, **40**, 7494-7500 (2006).
22. Vermeer, A. W. P., van Riemsdijk, W. H., and Koopal, L. K., "Adsorption of humic acid to mineral particles. 1. Specific and electrostatic interactions," *Langmuir*, **14**, 2810-2819 (1998).